









Article

Satellite and In Situ Monitoring of Chl-*a*, Turbidity, and Total Suspended Matter in Coastal Waters: Experience of the Year 2017 along the French Coasts

Francis Gohin ^{1,*}, Philippe Bryère ², Alain Lefebvre ³, Pierre-Guy Sauriau ⁴,
Nicolas Savoye ⁵, Vincent Vantrepotte ⁶, Yann Bozec ⁷, Thierry Cariou ⁸, Pascal Conan ⁹,
Sylvain Coudray ¹⁰, Gaëlle Courtay ¹¹, Sylvaine Françoise ¹², Anne Goffart ¹³,
Tania Hernández Fariñas ¹², Maud Lemoine ¹⁴, Aude Piraud ¹⁵, Patrick Raimbault ¹⁶ and
Michael Rétho ¹⁷

- ¹ Laboratoire d'écologie pélagique, IFREMER, DYNECO PELAGOS, CS 10070-29280 Plouzané, Brittany, France
 - ² Argans France, Etablissement de Brest, Le Grand Large Quai de la Douane, 29200 Brest, France; pbryere@argans.eu
 - ³ Laboratoire Environnement et Ressources de Boulogne-sur-mer, IFREMER, Quai Gambetta, BP 699, 62321 Boulogne-sur-mer, France; alain.lefebvre@ifremer.fr
 - ⁴ Littoral Environnement et Sociétés (LIENSs, UMR7266), CNRS, Univ. La Rochelle, 2 rue Olympe de Gouges, 17000 La Rochelle, France; pierre-guy.sauriau@univ-lr.fr
 - ⁵ EPOC, EPHE, UMR 5805, CNRS, Univ. Bordeaux, F-33600 Pessac, France; nicolas.savoye@u-bordeaux.fr
 - ⁶ Laboratoire d'Océanologie et de Géosciences LOG UMR8187, ULCO, Univ. Lille CNRS, 62930 Wimereux, France; vincent.vantrepotte@univ-littoral.fr
 - ⁷ Station Biologique de Roscoff, UPMC Univ. Paris 06, CNRS, UMR 7144 AD2M, Sorbonne Université, 29680 Roscoff, France; yann.bozec@sb-roscoff.fr
 - ⁸ Station Biologique de Roscoff, CNRS, Fédération de Recherche (FR2424), Sorbonne Université, 29680 Roscoff, France; cariou@sb-roscoff.fr
 - ⁹ Laboratoire d'Océanographie Microbienne (LOMIC), Sorbonne Université, UPMC (Paris VI), CNRS UMR 7621, 66650 Banyuls Sur Mer, France; pascal.conan@obs-banyuls.fr
 - ¹⁰ Laboratoire Environnement et Ressources Provence-Azur-Corse, IFREMER, Zone Portuaire de Brégaillon, CS20 330, CEDEX, 83507 La Seyne-sur-Mer, France; sylvain.coudray@ifremer.fr
 - ¹¹ IFREMER—UMR 5244 IHPE, Université de Montpellier, Place Eugène Bataillon, CC 80, CEDEX 5, 34095 Montpellier, France; gaëlle.courtay@ifremer.fr
 - ¹² Laboratoire Environnement et Ressources de Normandie, IFREMER, Av. Du Général de Gaulle, BP, 32-14520 Port en Bessin, France; Sylvaine.Francoise@ifremer.fr (S.F.); Tania.Hernandez.Farinas@ifremer.fr (T.H.F.)
 - ¹³ Laboratory of Oceanology, FOCUS Research Unit, Univ. Liège, Allée du 6 août, 11, B6c, 4000 Liège, Belgium; A.Goffart@uliege.be
 - ¹⁴ VIGIES, IFREMER, rue de l'Île d'Yeu, CEDEX 03, 44311 Nantes, France; maud.lemoine@ifremer.fr
 - ¹⁵ Laboratoire Environnement et Ressources des Pertuis Charentais, IFREMER, Avenue de Mus de Loup—Ronce les Bains, 17390 La Tremblade, France; aude.piraud@ifremer.fr
 - ¹⁶ Mediterranean Institute of Oceanography (MIO) UM 110, IRD, CNRS/INSU, Univ. Aix-Marseille, Université de Toulon, 13288 Marseille, France; patrick.raimbault@mio.osupytheas.fr
 - ¹⁷ Laboratoire Environnement et Ressources Morbihan/Pays de Loire, IFREMER, rue François Touleuc, 56100 Lorient, France; michael.retho@ifremer.fr
- * Correspondence: francis.gohin@ifremer.fr; Tel.: +33-298224315

Received: 22 July 2020; Accepted: 24 August 2020; Published: 28 August 2020



Abstract: The consistency of satellite and in situ time series of Chlorophyll-*a* (Chl-*a*), Turbidity and Total Suspended Matters (TSM) was investigated at 17 coastal stations throughout the year 2017. These stations covered different water types, from relatively clear waters in the Mediterranean Sea to moderately turbid regions in the Bay of Biscay and the southern bight of the North-Sea.

Satellite retrievals were derived from MODIS/AQUA, VIIRS/NPP and OLCI-A/Sentinel-3 spectral reflectance. In situ data were obtained from the coastal phytoplankton networks SOMLIT (CNRS), REPHY (Ifremer) and associated networks. Satellite and in situ retrievals of the year 2017 were compared to the historical seasonal cycles and percentiles, 10 and 90, observed in situ. Regarding the sampling frequency in the Mediterranean Sea, a weekly in situ sampling allowed all major peaks in Chl-*a* caught from space to be recorded at sea, and, conversely, all in situ peaks were observed from space in a frequently cloud-free atmosphere. In waters of the Eastern English Channel, lower levels of Chl-*a* were observed, both in situ and from space, compared to the historical averages. However, despite a good overall agreement for low to moderate biomass, the satellite method, based on blue and green wavelengths, tends to provide elevated and variable Chl-*a* in a high biomass environment. Satellite-derived TSM and Turbidity were quite consistent with in situ measurements. Moreover, satellite retrievals of the water clarity parameters often showed a lower range of variability than their in situ counterparts did, being less scattered above and under the seasonal curves of percentiles 10 and 90.

Keywords: satellite; coastal monitoring; Chlorophyll-*a*; Total suspended matter; turbidity

1. Introduction

Since the launch of SeaWiFS in August 1997, marine reflectance data at about 1 km resolution have been provided by space agencies without interruption. As the ocean color sensors have been designed primarily for a better knowledge of the carbon cycle at global range, the algorithms for processing marine reflectance, such as the OC4 algorithm of NASA [1], were initially designed for open waters where the optic components are those of pure water and phytoplankton, alive or through detrital products. The coastal case was more difficult as exogenous CDOM (Colored Dissolved Organic Matter) and/or mineral suspended matters, resulting from resuspension by waves or by strong tidal current, hamper the application of standard open sea algorithms. Many regional algorithms have been developed for coastal seas. Among them the Ifremer OC5 algorithm, derived from OC4, has been largely applied to SeaWiFS, MODIS, VIIRS, MERIS marine reflectance with numerous validations in coastal waters of the eastern Atlantic Ocean [2–5] and in the western Mediterranean Sea [6,7]. It is currently applied at global scale through the OC-CCI (Ocean Color-Climate Change Initiative) and GlobColour products of the CMEMS (Copernicus Marine Environment Centre) [8,9]. After an initial phase of validation based on data obtained from cruises in clear or moderately turbid waters [10], the adjustment of the algorithm is currently performed from validations on coastal stations [11], providing different sensor-specific Look-Up-Tables. The calibration of the algorithm is obtained by minimization between the satellite and in situ seasonal cycles of Chlorophyll-*a* (Chl-*a*), Turbidity and Total Suspended Matter (TSM) derived from a large number of observations at coastal stations [11]. Moreover, the performance of the Chl-*a* algorithm has also been assessed, more conventionally, from accurate match-ups, with restricted spatial and temporal deviation between in situ observations and satellite retrievals [4,12,13]. However, the effective contribution of the satellite retrievals to the knowledge of the short term (weekly) dynamics of the coastal environment has not been evaluated in the context of existing conventional in situ networks.

Our purpose is therefore to assess the overall performance of the space and in situ monitoring to observe the dynamics in Chl-*a*, Turbidity and TSM throughout the year in coastal waters. To have a representative data set of the coastal French waters, 17 stations have been selected, from the Mediterranean Sea to the southern North-Sea (Figure 1). Different optical constraints are encountered in these clear or moderately turbid waters that are also associated with various atmospheric backgrounds through seasons and locations, and diverse cloud coverages, this latter being much lower over the Mediterranean Sea than along the Atlantic seaboard. Although the literature generally underlines the

limitation of the satellite retrievals in coastal waters, the in situ datasets are not free of uncertainty and variability in the methods, frequencies, and quality controls. For assessing the range of variability of both data types we will consider some elementary statistics, as the seasonal cycles of the average, percentiles 10 and 90. The overall coherence of the satellite and in situ datasets will be considered, not only parameter by parameter, as already mentioned, but also between parameters. Turbidity and TSM are not measured in situ at all the stations while satellite retrievals are provided equivalently for these two parameters. It is, therefore, not just the performance of the in situ or satellite monitoring that we aim to assess in this study but also the capacity of both methods to improve collectively our insight into the variability of the marine coastal environment. This could also give indications to design an optimal integrated network, notably when in situ data are scarce or missing, to fulfill the regulatory requirements of the Oslo Paris convention [14], the Water Framework Directive [15] and the Marine Strategy Framework Directive [16]. The question of how best we can merge large datasets of satellite data into conventional observing systems for assessing quantitatively the water quality is an open question that needs to be explored in detail [2,17]. To simplify the representation of the satellite and in situ datasets a single year, the year 2017, will be considered in this study which aims at identifying the main issues for building up an integrated monitoring system in coastal waters.

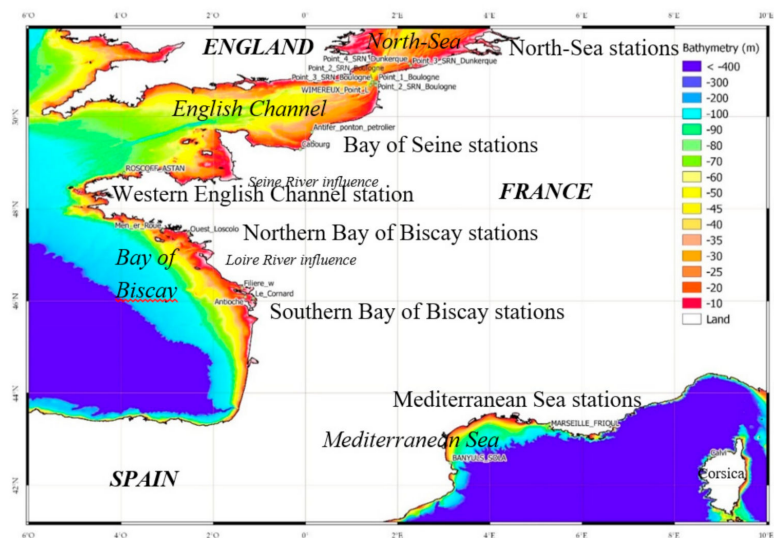


Figure 1. Maps of the selected 17 stations and bathymetric background.

2. Materials and Methods

2.1. In Situ Data

2.1.1. Local, Regional or National Networks

Most of the in situ data were provided by the SOMLIT (Service d'Observation en Milieu Littoral) [18] operated and funded by CNRS (Centre National de la Recherche Scientifique, Paris, France) and French universities, and by the REPHY/network managed by Ifremer [19]. The Dunkerque and Boulogne stations (the northernmost stations) belong to the SRN (Suivi Régional des Nutriments) network, funded by the Water Agency Artois-Picardie [20] in order to follow the environmental conditions at the origin of eutrophication characterized by recurrent spring blooms of the Pymnesiophyceae *Phaeocystis globosa*. SRN data are embedded in the REPHY network. The data in the Bay of Seine, at Antifer and Cabourg stations, were provided by the RHLN (Réseau Hydrologique du Littoral Normand), funded by the Water Agency Seine-Normandie and also embedded in the REPHY network. The SRN network provided Chl-*a*, TSM and Turbidity (NTU). The other REPHY stations collected Chl-*a* and Turbidity data whereas the SOMLIT stations sampled Chl-*a* and TSM data. The northern stations

(Dunkerque, Boulogne, and Wimereux in Figure 2) are located along transects enabling the observation of cross-shore gradients in Chl-*a*, TSM and Turbidity. The sampling of Chl-*a* at the Calvi station was funded by Ifremer and by the Territorial Community of Corsica and the Rhone-Mediterranean and Corsica Water Agency within the framework of the Starecapmed program. Some of these data are also embedded within the REPHY. Analyses were funded by the University of Liège (Belgium) and Ifremer.

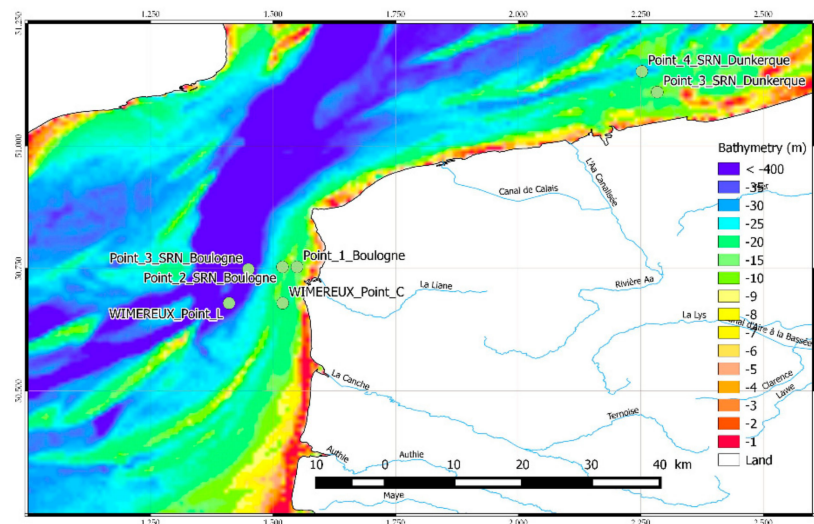


Figure 2. Zoom on the northern stations along three cross-shore transects: Dunkerque 3 and 4, Boulogne 1, 2 and 3, and Wimereux C and L.

2.1.2. Diverse Environmental Conditions

The main characteristics of the different stations are given in Table 1. Fourteen Atlantic stations, from the Bay of Biscay to the southern North-Sea, are located in nutrient-rich waters whereas the Mediterranean stations are in oligo- to mesotrophic waters. The Calvi station is a well-preserved site with a phytoplankton bloom occurring during the winter-spring period in relation to winter wind events enabling the replenishment of surface nutrients [21].

At the SOMLIT stations, the Particulate Organic Matter (POM) is dominated by phytoplankton, showing little influence of rivers in the organic matter, except at Antioche and Banyuls-Sola where the terrestrial component of POM can reach up to 20 and 10% of the total POM respectively [22,23]. A similar observation could be made on the REPHY stations; they are under the influence of rivers in term of nutrients and salinity but not strongly enough to have a significant part of organic materials of terrestrial origin. The stations are not located in transitional (estuarine) waters according to the classification of the European Directives. The stations of the southern Bay of Biscay, FilièresWest, le Cornard and Antioche are located in areas of a large mussel and oyster farming industry with strong interaction between shellfish population and water properties [24,25].

The observations are made at surface (0.5–1 m) and at High Water (± 1 h for SOMLIT and ± 2 h for REPHY) in low to moderate spring tides. Samples volumes may vary between 0.1 to 2 L depending on in situ conditions. The oldest data used for calculating the historical statistics are from 1998. The most recent ones are from 2018 or 2019 for some stations.

Table 1. Characteristics of the selected stations.

Region	Station	Network	Water Depth	Parameters	Period in Our Dataset	Sampling Frequency	Tidal Range	Trophic Status
North-Sea	Dunkerque	REPHY/SRN	12 m	Chl- <i>a</i> , TSM, Turbidity	1998–2018	bimonthly during the productive period, then monthly	macro-tidal	eutrophic
	Point 3 Point 4		14 m					
Eastern English Channel	Boulogne	REPHY/SRN	20 m	Chl- <i>a</i> , TSM, Turbidity	idem	idem	idem	idem
	Point 1, Point 2 Point 3		20 m 30 m					
	Wimereux	SOMLIT	21m 50m	Chl- <i>a</i> , TSM	1998–2018 2009–2018	idem	idem	idem
Bay of Seine	Cabourg	REPHY/ RHLN	10 m	Chl- <i>a</i> , Turbidity	2001–2018	bimonthly	idem	idem
	Antifer Ponton Pétrolier	REPHY/ RHLN	30 m	Chl- <i>a</i> , Turbidity	2001–2018	bimonthly since 2015, monthly before	idem	idem
Western English Channel	Roscoff Astan	SOMLIT	60 m	Chl- <i>a</i> , TSM	1998–2019	bimonthly	macro-tidal	idem
Northern Bay of Biscay	Men er Roue	REPHY	10 m	Chl- <i>a</i> , Turbidity	1998–2019 2008–2019	bimonthly	meso-tidal	meso-trophic
	Ouest-Loscolo	REPHY	10 m	Chl- <i>a</i> , Turbidity	1998–2019 2008–2019	idem	idem	eutrophic
Southern Bay of Biscay	Filières-West	REPHY	20 m	Chl- <i>a</i> , Turbidity	1998–2018 2008–2018	idem	meso-tidal	meso-trophic
	Le Cornard	REPHY	13 m	Chl- <i>a</i> Turbidity	1998–2019 2008–2019	idem	idem	idem
	Antioche	SOMLIT	40 m	Chl- <i>a</i> , TSM	2011–2019	bimonthly	macro-tidal	idem
Mediterranean Sea	Banyuls-Sola	SOMLIT	27 m	Chl- <i>a</i> , TSM	1998–2019	weekly	micro-tidal	meso-trophic
	Marseille- Frioul	SOMLIT	60 m	Chl- <i>a</i> , TSM	1998–2019	bimonthly	micro-tidal	oligo-trophic
	Calvi PhytoCly site	REPHY/Univ. Liège/Stareso	10–38 m	Chl- <i>a</i>	2006–2018	biweekly	micro-tidal	oligo-trophic

More details on the SOMLIT measurements of Chl-*a* and TSM are given by [22,23]. Methods for measuring Chl-*a*, TSM and Turbidity in the SRN network are described in [20]. Turbidity measured at the SRN stations follows the standard 181.1 of USEPA (1980) whereas the other measurements at the REPHY stations follow the newest standard ISO 7027. References for the measurements of Chl-*a* and Turbidity for the REPHY stations are provided in [19]. Most of the Chl-*a* data were obtained by fluorimetry. Chl-*a* was extracted using 90% acetone and analyzed by fluorescence [26] and TSM was obtained from water samples filtered through pre-combusted (4 h–450 °C) GF/F filters following [27]. All network laboratories contributed to intercalibration exercises under the behalf of Ifremer, SOMLIT and Aquaref consortium.

2.2. Satellite Data

Daily MODIS-Aqua, VIIRS and OLCI-A normalized water-leaving radiance was projected on an “Atlantic” grid at a resolution of 1 km (Level 3 product). The normalized water-leaving radiance was derived from the standard marine remote-sensing reflectance (Level 2 products) provided by NASA for MODIS and VIIRS and by EUMETSAT for OLCI-A.

2.2.1. Chl-*a* Concentration

Chl-*a* concentration was obtained from the application of 3 sensor-specific OC5 Look-Up Tables (LUT) to spectral remote-sensing radiance [10]. To derive Chl-*a* the LUTs were applied to a triplet of entries: the maximum ratio of reflectance Blue/Green used by the OC4 algorithm and the normalized water-leaving radiances at 412 and at 560 nm. For OLCI-A. The MODIS and VIIRS LUT have been defined in 2015 and kept unchanged. The OLCI-A LUT was a preliminary LUT that will be improved when a longer time series of OLCI-A data will be available.

2.2.2. Total Suspended Matter

The non-algal part of TSM was estimated using the semi-analytical algorithm defined in [28]. In this semi-analytical method, absorption and backscattering by phytoplankton are derived from preliminary estimations of Chl-*a* concentration by OC5. Then, non-algal SPM are obtained from radiance at 550 nm and 670 nm. Depending on the level of the retrieved non-algal SPM using both radiances, the final non-algal SPM was chosen at 550 nm if both non-algal SPM concentrations (estimated from radiance at 550 nm and 670 nm) were less than 4 g m⁻³. In the cases where non-algal SPM concentration (estimated from radiance at 550 nm and 670 nm) was more than 4 g m⁻³, non-algal SPM derived from radiance at 670 nm was chosen.

Total Suspended Matter was estimated from non-algal SPM and Chl-*a* using (1):

$$\text{TSM} = \text{non-algal SPM} + 0.234\text{Chl-}a^{0.57} \quad (1)$$

In (1) TSM is expressed in g m⁻³ and Chl-*a* in mg m⁻³.

2.2.3. Turbidity

Turbidity was estimated from SPM following 2 formula depending on the sensor [11]. For the first generation of sensors following the standard 181.1 of USEPA (1980):

$$\text{Turbidity (NTU)} = 0.54 \text{ TSM} \quad (2)$$

For the second generation of sensor following the standard ISO 7027:

$$\text{Turbidity (FNU)} = 1.28 \times 0.54 \text{ TSM} \quad (3)$$

These water clarity products have been evaluated in detail along the French coasts [11] and at the location of the Liverpool Bay mooring in the coastal waters of the Irish Sea [29].

Chl-*a*, Turbidity and TSM corresponding to the pixel of the “Atlantic grid” (1.2 km) where the stations are located were selected without further averaging.

2.3. Statistics at the Stations

Basic statistics were calculated to provide the baselines of the historical in situ yearly cycle. The mean yearly cycle was calculated from two-week averages at every station. All the data collected at each station (beginning in the year 1998 when SeaWiFS was launched, see Table 1) were used to calculate the mean and percentiles 10 (P10) and 90 (P90) for fortnights 1 to 26 following the procedure described in [11]. The historical in situ mean, P10 and P90 were also evaluated over the productive period (March to October for the Atlantic stations, January to December for those in the Mediterranean Sea). The mean and P90 were also provided over the productive period of the year 2017 for the in situ, MODIS, VIIRS and OLCI-A datasets. The percentile 90 of Chl-*a* over the productive period has been chosen in our investigations as it is one of the major metrics proposed to assess the environmental status of coastal waters in the European Water Framework Directive and in the Marine Strategy Framework Directive.

3. Results

Although the aim of this work was not the calibration of the satellite algorithms, a slight modification of some parameters in the TSM algorithm has been carried out. This modification has been made in the equations of the non-algal SPM algorithm, particularly in order to obtain better fits for low TSM values, as those encountered in the Mediterranean Sea.

Graphs of the time series of Chl-*a*, Turbidity and TSM were generated for the years 2016 to 2018 but only graphs of the year 2017 are shown for all stations (Figures 3–12). The 2018 graphs (exceptionally the 2016 graphs) are used in the discussion to investigate different issues observed at some stations in 2017. In situ measurements of turbidity at the REPHY/SRN stations (Dunkerque and Boulogne transects) have been corrected by a factor 1.28 for consistency with other Turbidity measurements that follow the standard ISO 7027 (Equation (3)).

3.1. Southern North-Sea

Figure 3 shows the satellite-derived retrievals and the in situ observations in Chl-*a*, SPM, and Turbidity for the year 2017 at the two stations of the Dunkerque transect in the North-Sea. The P90 of the year for each sensor and from the in situ measurements are also indicated on the figure, together with the P10, P90 and the average of the historical in situ data during the productive season (March to October). The satellite retrievals are more numerous than the in situ observations and the percentile 90 derived from these latter, obtained from a lower number of data, are statistically less reliable when calculated over a single year. The satellite P90 in Chl-*a*, around 12 and 8 g m⁻³ for Point 3 (coastal) and 4 (offshore), respectively, are close to those historically observed in situ. The most striking feature on these graphs, with possible consequence in the assessment of the eutrophic status through the level in Chl-*a*, is the spring peak in April. At that time several satellite retrievals are above the in situ P90 line. Satellite and in situ TSM (Figure 3b,e) and Turbidity (Figure 3c,f) are in good agreement. The satellite retrievals in Turbidity appear nevertheless closer to in situ measurements. Both datasets exhibit also a Turbidity under average in March and April 2017, indicating clearer waters and better conditions for the onset of the spring bloom.

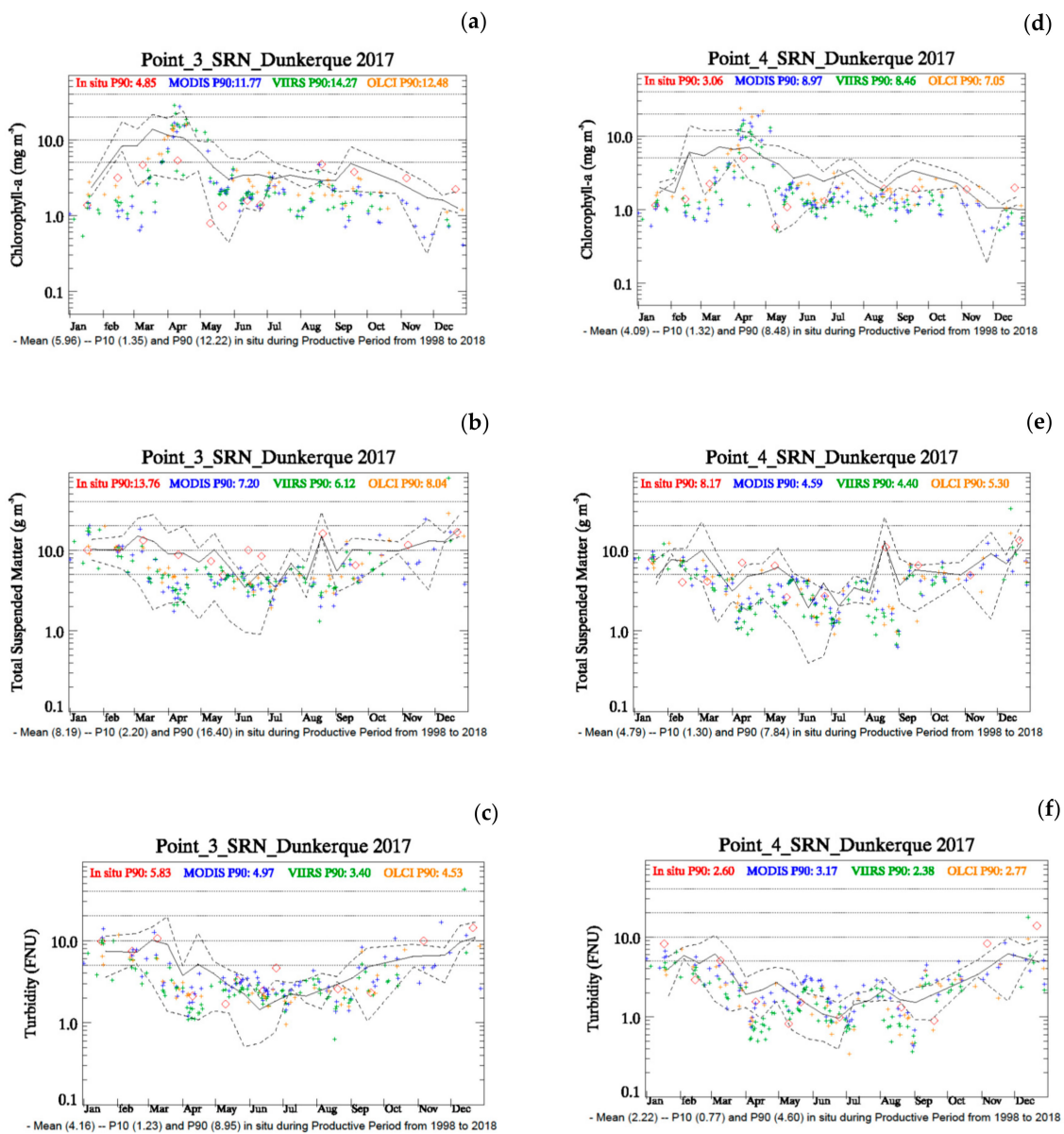


Figure 3. Chl-*a* (a,d), TSM (b,e) and Turbidity (c,f) in the southern North-Sea. In situ and satellite percentiles of year 2017 are indicated in the upper part of the graphs; the in situ historical mean, P10 and P90, calculated over the productive period, are indicated under the time axis.

3.2. Eastern English Channel

Very similarly to the Dunkerque time series, a peak in Chl-*a* is observed in April at Boulogne Point 1, Point 2, and Wimereux Point C, i.e., the sites the closest to the coast (Figure 4a,b,d).

Except for the period corresponding to the spring peak, around the end of April, the 2017 Chl-*a* levels are much lower than the historical average line at all the stations in the eastern English Channel and whatever the data origin. This confirms the results by [5] concerning a decline in the Chl-*a* concentration during the post-bloom stage in the Eastern English Channel over the period 1998–2017. Some in situ TSM data appear particularly high at Boulogne Point 1 (Figure 4f). Many of these high observations are around or above the historical P90 line. For the year 2017, the satellite and in situ P90 of TSM are lower than average at Wimereux_Points C and L (Figure 4i,j) whereas in situ percentiles 90 are higher along the Boulogne transect (Figure 4f–h). There is an apparent inconsistency of the dynamics of the in situ observations of TSM despite the geographic proximity of these stations whereas Turbidity statistics along the Boulogne transect (Figure 5) are close to the average conditions (6.42, 4.22, and 2.43 FNU for Point 1, 2, and 3, respectively).

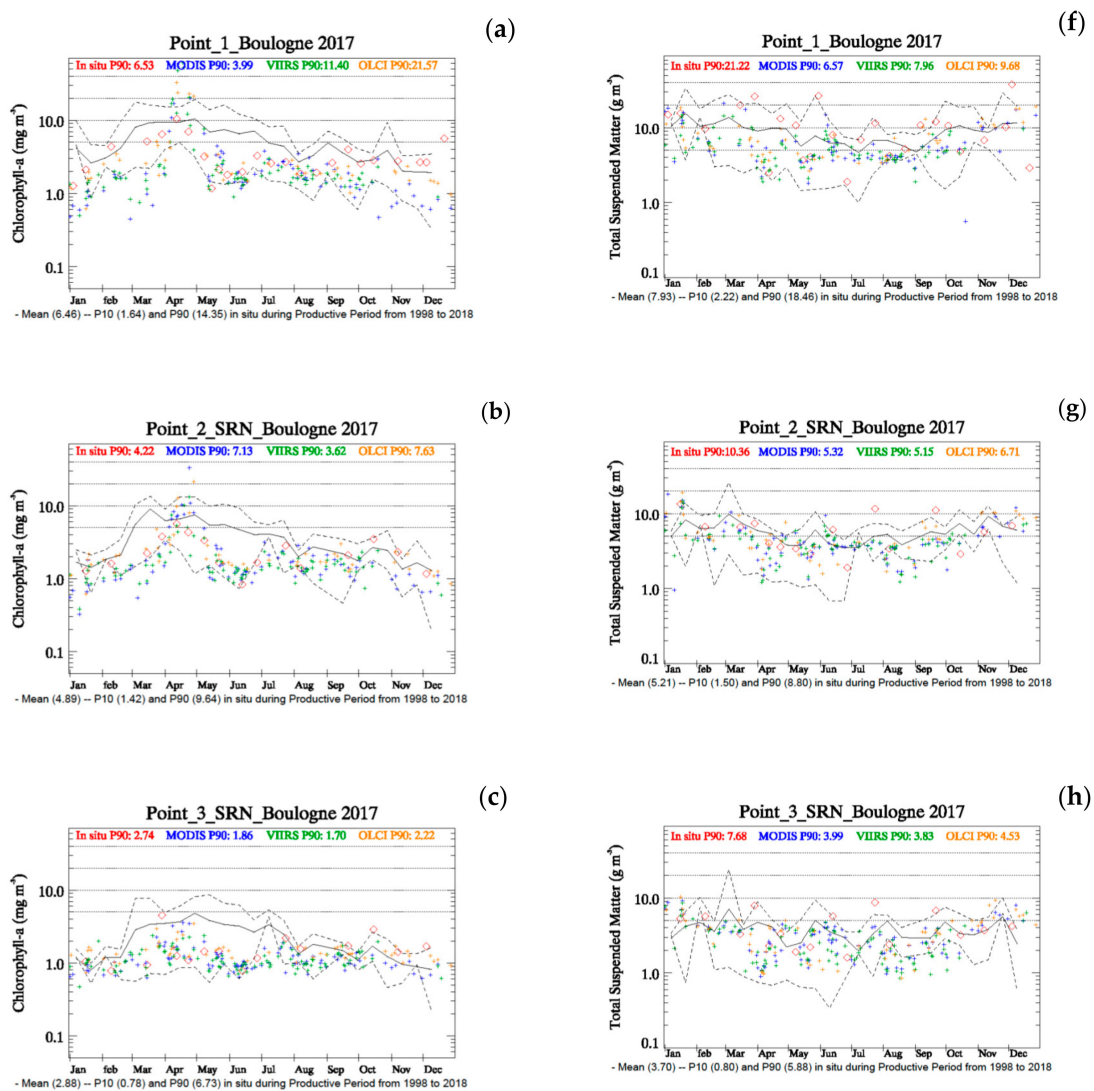


Figure 4. Cont.

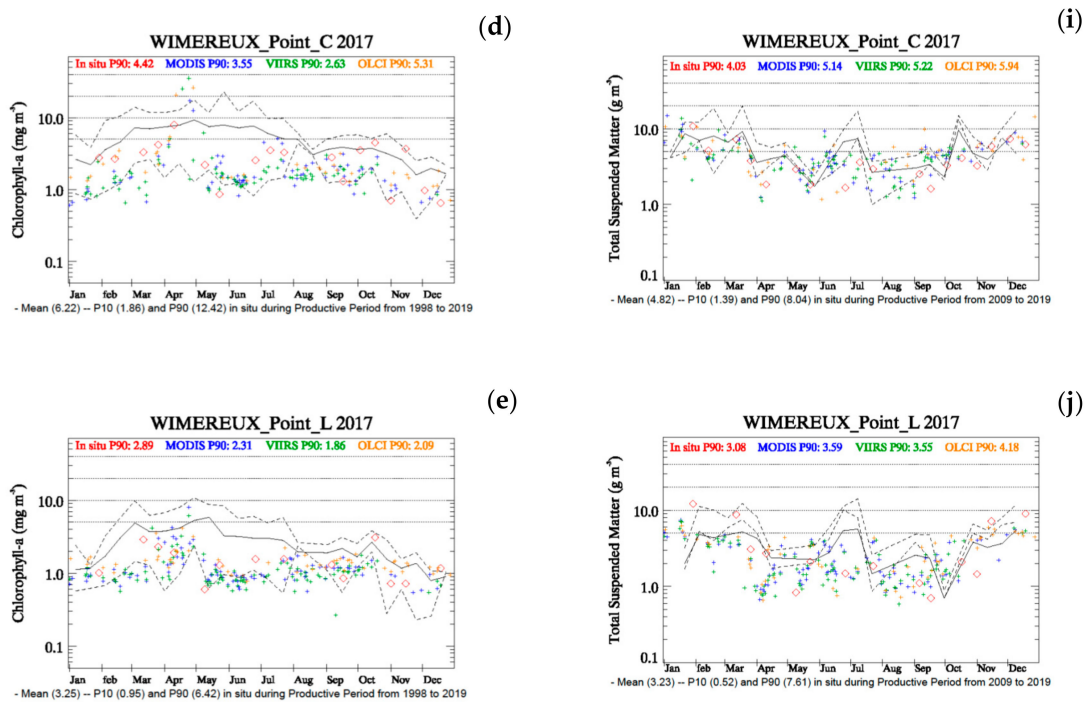


Figure 4. Chl-*a* (a–e) and TSM (f–j) in the eastern English Channel. In situ and satellite percentiles of year 2017 are indicated in the upper part of the graphs; the in situ historical mean, P10 and P90, calculated over the productive period, are indicated under the time axis.

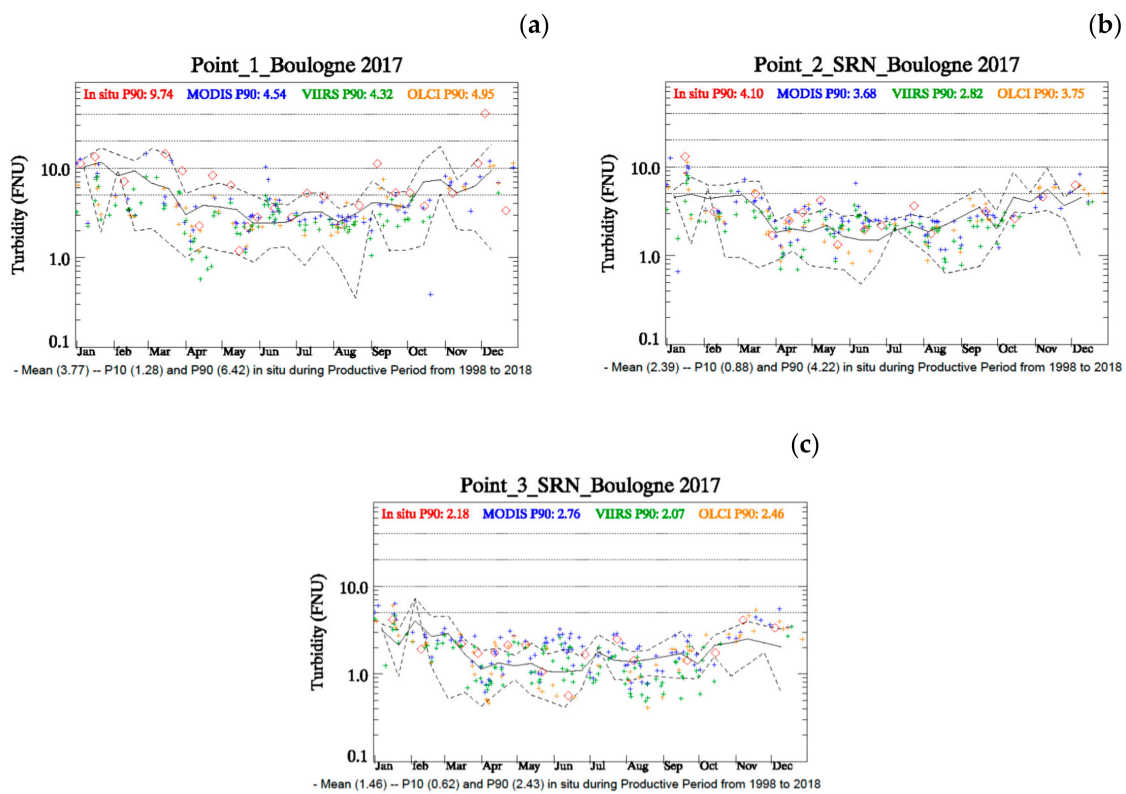


Figure 5. Turbidity along the Boulogne transect (a: Point 1; b: Point 2; c: Point 3). In situ and satellite percentiles of year 2017 are indicated in the upper part of the graph; the in situ historical mean, P10 and P90, calculated over the productive period, are indicated under the time axis.

3.3. Bay of Seine and Western English Channel

Since stations at Cabourg and Antifer Ponton Petrolier (the petroleum wharf of the Antifer Harbor) are very close to the coast, satellite retrievals are less numerous than at any other station within our dataset (Figure 6a,b,d,e). This is due to the occurrence of numerous failures in the processing of the Top of Atmosphere radiance leading to flagged reflectance. Despite this proximity to shore, the observations obtained from space and in situ exhibit consistent patterns in 2017. The Chl-*a* concentrations lie under the historical line, similarly to the stations of the Eastern English Channel. However, contrarily to the stations in the Eastern English Channel, there is no obvious spring peak at Cabourg and Antifer as these stations are under the influence of the plume of the river Seine and its permanent nutrient loads flowing into the area throughout spring and summer. Nevertheless, at all stations from the central to the Eastern English Channel, a lower level in phytoplankton biomass, compared to average, is recorded in 2017 [5]. Temporal variability of turbidity is particularly high in situ at Antifer (Figure 6d). This phenomenon could be explained by a higher variability at small range in the harbor. Chl-*a* at Roscoff Astan is quite low throughout the year (Figure 6c) but high TSM are observed in situ in summer without correspondence in satellite retrievals (Figure 6f). We can discard any physical cause (as tide) to explain these very high levels as these high levels were not observed in 2018 (Figure 7). Affected by these elevated TSM, the historical average line in situ is probably too high in summer as already observed in [11]. A slight positive bias in the satellite Chl-*a* during the winter months is also observed at Roscoff Astan.

3.4. Bay of Biscay

At stations Men er Roue and Ouest-Loscolo, some high Chl-*a* concentrations are observed in spring within the MODIS and VIIRS retrievals (Figure 8a,b). On the contrary, several in situ data are in the vicinity of the P10 historical line. A lower variability in the Chl-*a* observations (Figure 8c–e) is observed at the turbid stations of the southern Bay of Biscay (Filières-West, Le Cornard and Antioche). In these waters, some OLCI-A retrievals appear to be particularly high in autumn and summer when waters are turbid. Despite different variabilities in the retrievals, all the P90 calculated over the productive period of 2017 are lower than average at all the Bay of Biscay stations. This is particularly true at the Filières-West station from March to May. In turbidity, the satellite retrievals appear much more stable than their in situ equivalents at Men er Roue and Ouest-Loscolo. The high scatter in the in situ turbidity measurements at surface, compared to historical statistics, may be due to the change of method in 2016 when a multi-parameter profiler was used. However, the main discrepancy in the time series is observed at Antioche where the satellite time series show a significant positive bias compared to the in situ measurements in 2017 (Figure 8j) and 2018 (Figure 9).

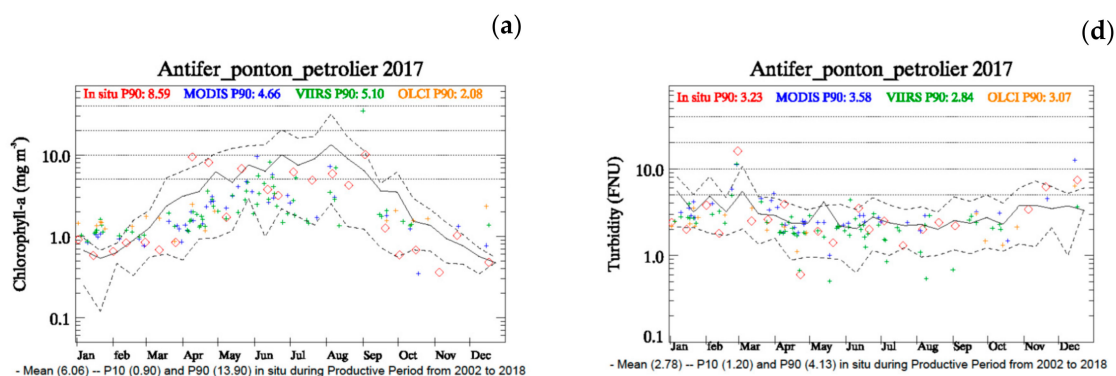


Figure 6. Cont.

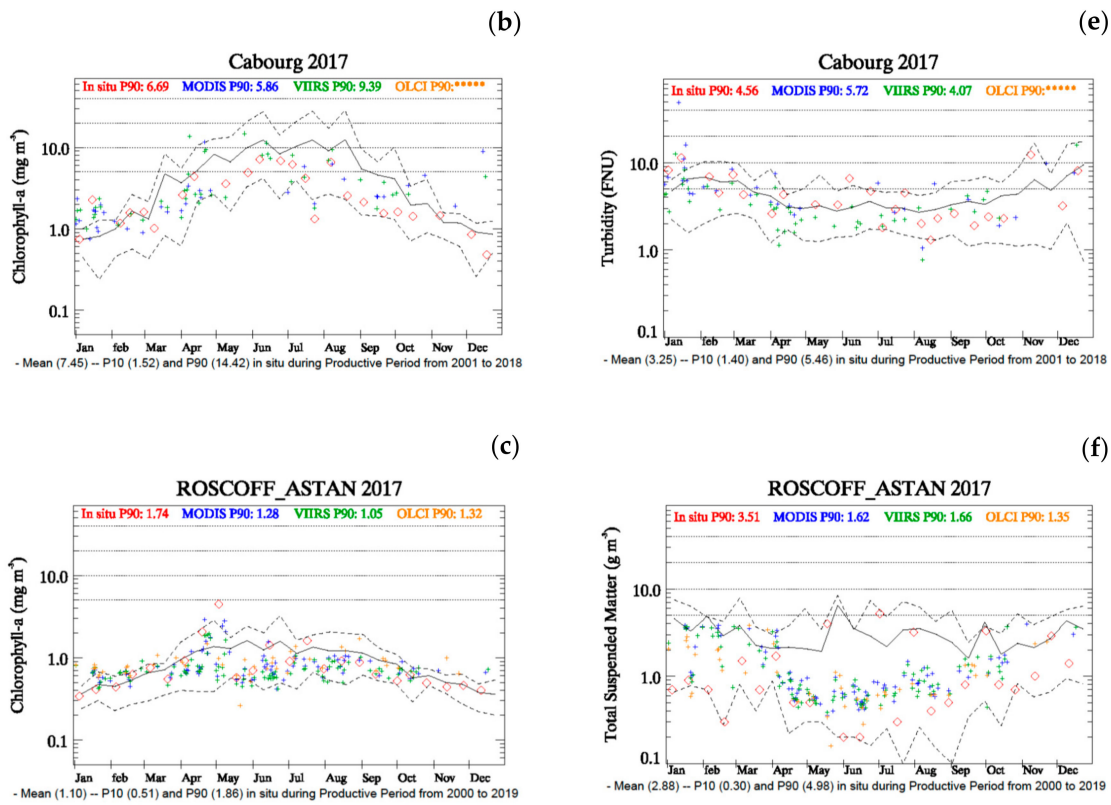


Figure 6. Chl-*a* (a–c), Turbidity (d,e) or TSM (f) in the Bay of Seine (Antifer and Cabourg) and in the western English Channel (Roscoff Astan). In situ and satellite percentiles of year 2017 are indicated in the upper part of the graphs; the in situ historical mean, P10 and P90, calculated over the productive period, are indicated under the time axis.

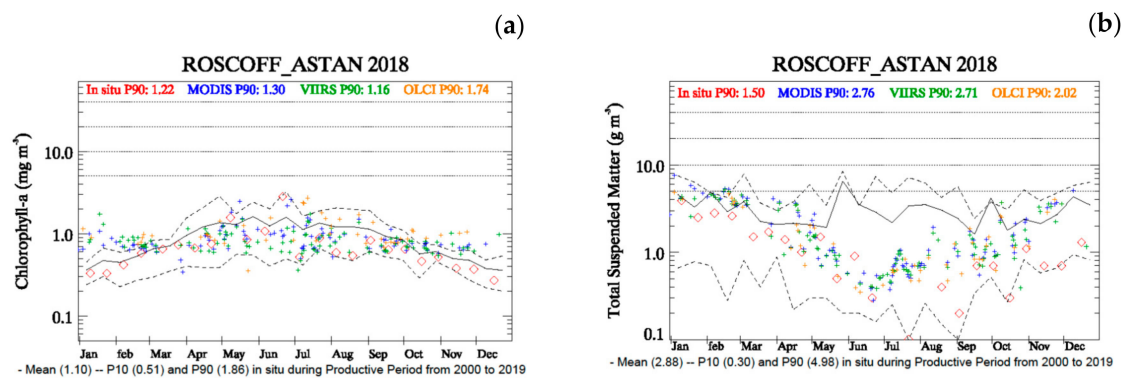


Figure 7. Chl-*a* (a) and TSM (b) at Roscoff Astan in 2018. In situ and satellite percentiles of year 2018 are indicated in the upper part of the graphs; the in situ historical mean, P10 and P90, calculated over the productive period, are indicated under the time axis.

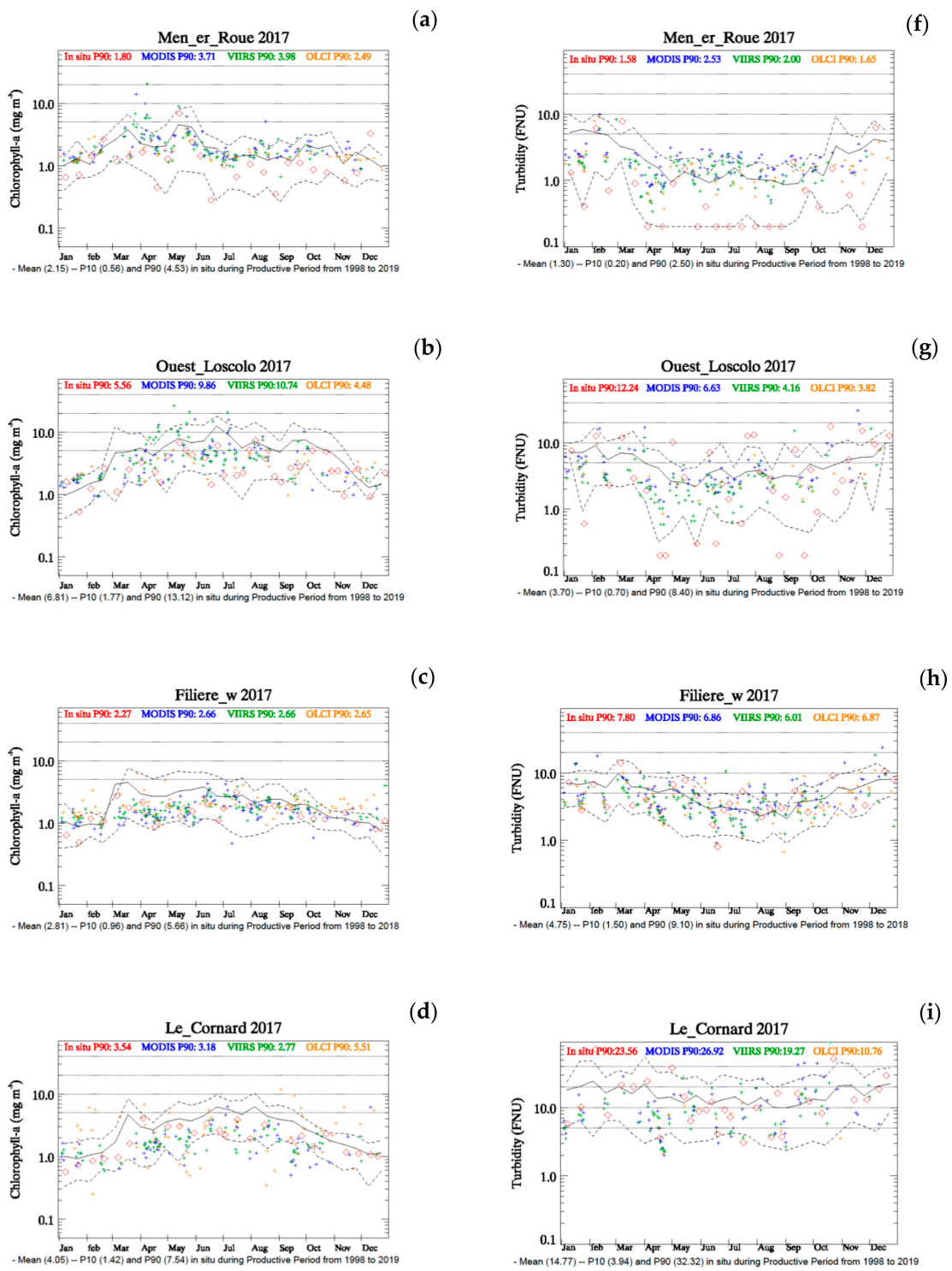


Figure 8. Cont.

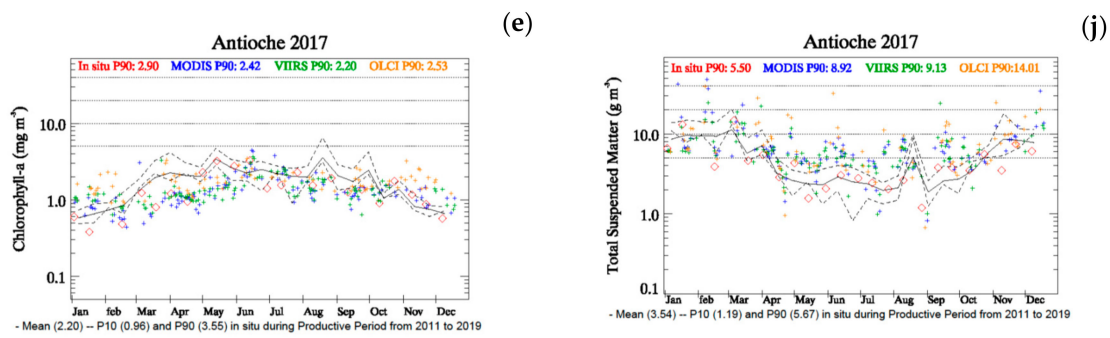


Figure 8. Chl-*a* (a–e), Turbidity (f–i) or TSM (j) in the Bay of Biscay. In situ and satellite percentiles of year 2017 are indicated in the upper part of the graphs; the in situ historical mean, P10 and P90, calculated over the productive period, are indicated under the time axis.

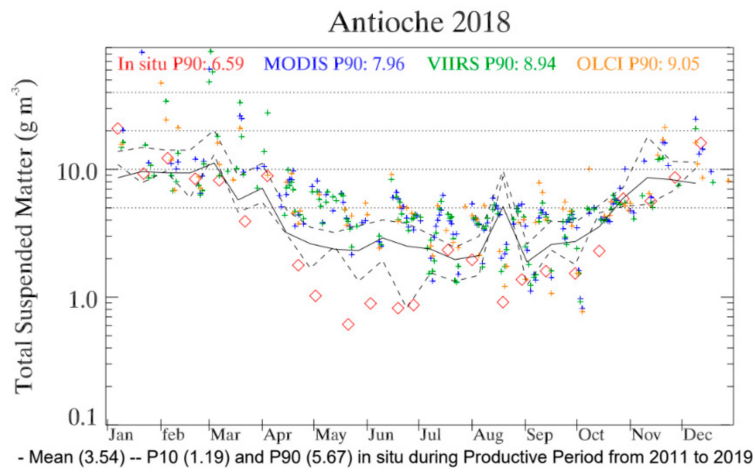


Figure 9. TSM at Antioche in 2018. In situ and satellite percentiles of year 2018 are indicated in the upper part of the graph; the in situ historical mean, P10 and P90, calculated over the productive period, are indicated under the time axis.

3.5. Mediterranean Sea

On overall, all the time series in Chl-*a* are in excellent agreement (Figure 10). The weekly sampling frequency appears to be particularly adequate to catch winter and autumn peaks at Banyuls-Sola (Figure 10a). However, some outliers are visible in situ among the large set of data collected at the Calvi station but both datasets capture a relatively high bloom in March followed by levels lower than average in spring (Figure 10c). The discrepancy is higher in TSM at Banyuls and Marseille (Figure 10d,e). In the summer months the satellite retrievals are lower at Banyuls but, looking at the 2018 situation (Figure 11), it is not a systematic artifact from the satellite method. At Marseille-Frioul, the satellite retrievals are systematically lower than the in situ observations, in 2017 and 2018. These records obviously reveal a minimum threshold of TSM of about 0.4 g m^{-3} under which the satellite method is poorly sensitive (Figure 10e).

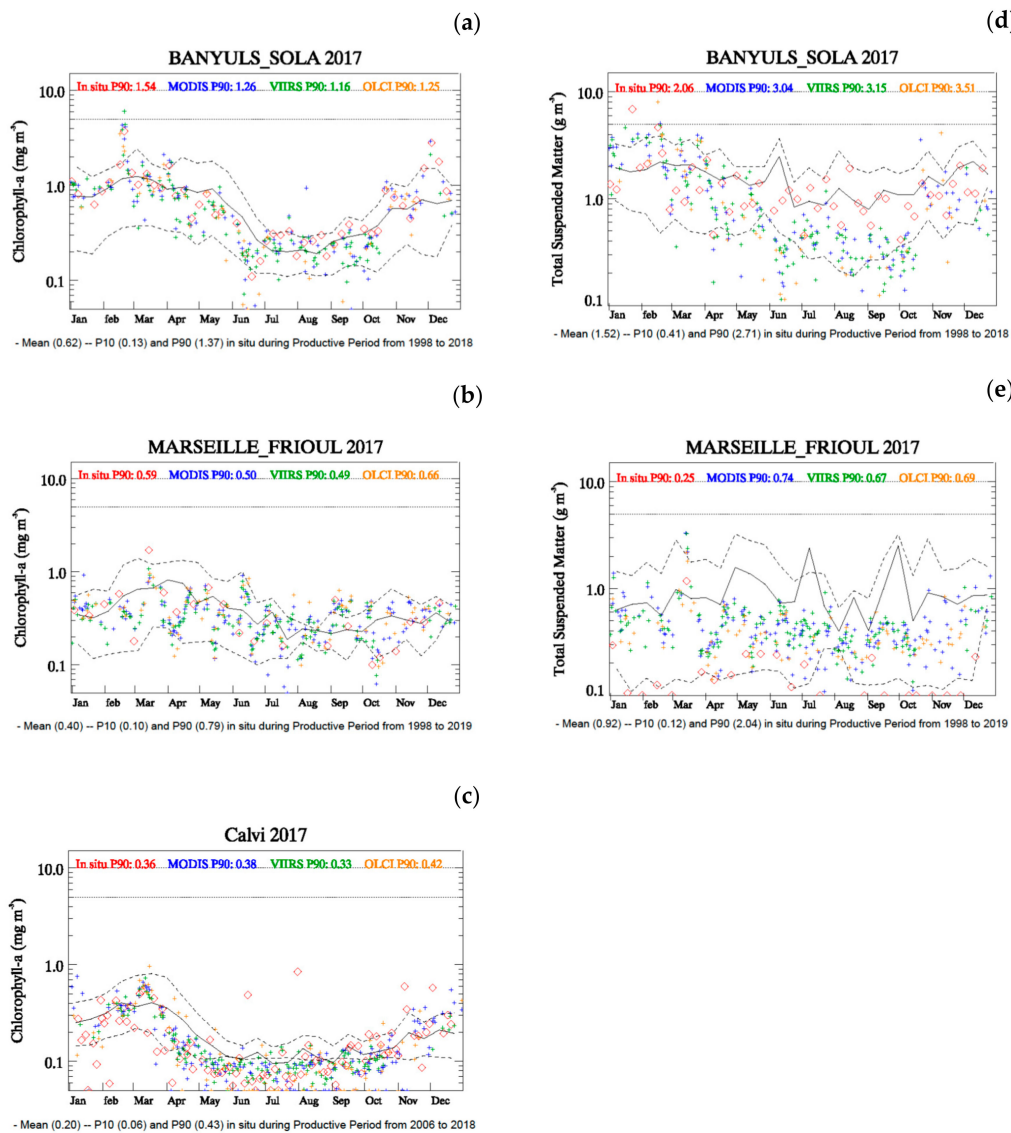


Figure 10. Chl-*a* (a–c) and TSM (d, e) in the Mediterranean Sea. In situ and satellite percentiles of year 2017 are indicated in the upper part of the graphs; the in situ historical mean, P10 and P90, calculated over the productive period, are indicated under the time axis.

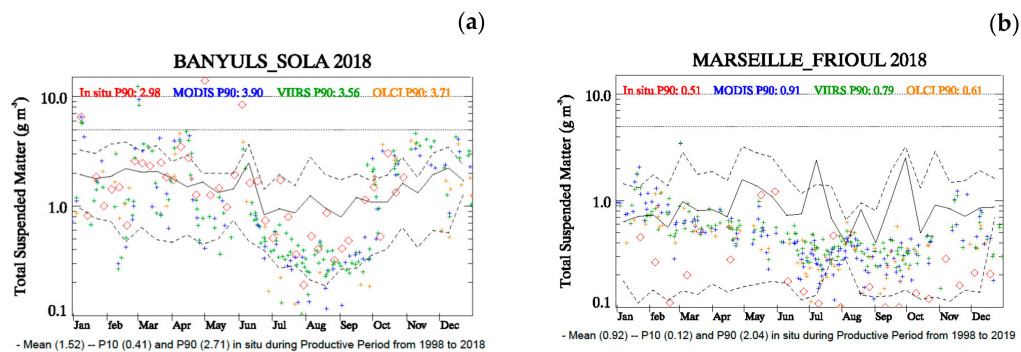


Figure 11. TSM at Banyuls-Sola (a) and Marseille-Frioul (b) in 2018. In situ and satellite percentiles of year 2018 are indicated in the upper part of the graphs; the in situ historical mean, P10 and P90, calculated over the productive period, are indicated under the time axis.

4. Discussion

4.1. Similarities and Discrepancies between the Satellite and In Situ Datasets

Our present results confirm an overall good agreement between the satellite-derived and in situ observations of Chl-*a*. The highest agreement is observed at the Banyuls station in the Mediterranean Sea. Therefore, the algorithm is robust enough to retrieve the Chl-*a* concentration over a wide range of water types, including western Mediterranean waters, between 0.2 mg m^{-3} and about 20 mg m^{-3} . Both satellite and in situ Chl-*a* concentration are lower than average during the productive period of the year 2017 in the central and eastern English Channel. However the spring peak remains as high as ever at all the Atlantic stations where it is observed. The satellite algorithm retrieves TSM and Turbidity above a threshold of about 0.4 g m^{-3} and 0.25 FNU respectively with deviations from the in situ measurements that can be relatively high, particularly in SPM. Many reasons may explain these discrepancies.

4.1.1. Error Source in the In Situ Measurements of Chl-*a*

In our in situ samples, Chl-*a* is mainly determined by fluorimetry which is known to under- or over-estimate Chl-*a* because of the overlap of the absorption and fluorescence bands of co-occurring Chl-*b* and *c*, chlorophyll degradation products and accessory pigments [30]. The major differences with the real Chl-*a* concentration, as derived from HPLC (High Performance Liquid Chromatography), could occur in autumn and winter when the content in degradation products is relatively high in the water.

4.1.2. Error Source in the Satellite-Derived Chl-*a*

As is the case with the fluorimetric method, the satellite algorithm is sensitive to the absorption coefficient of the algal cell in the blue band; which is depending on the cell size (“packaging effect”) and pigment composition [31]. Therefore, any variation from the “average” environment is likely to affect the Chl-*a* retrievals. A second source of error at the northern stations (English Channel and North-Sea) during the dark months (November to January) can be attributed to high solar zenith angles. A lower signal/noise ratio in water-leaving radiance is known to have a significant impact on the detection of Chl-*a* changes [32]. However, at that time of the year, the complexity of the coastal environment is so high that the in situ Chl-*a* derived from fluorimetry could be overestimated, making questionable any conclusion on the accuracy of the satellite retrievals based on comparison to these data at these locations in winter.

The highest discrepancy between the satellite and in situ time series of Chl-*a* is nevertheless observed during the spring peaks over the Atlantic seaboard, as exhibited along the Dunkerque and Boulogne transects (Figure 3 and Figure 4) but also in summer at Men er Roue and Ouest-Loocolo in the Bay of Biscay (Figure 8a,b). These events always occur in specific atmospheric conditions characterized by condensation droplets or high humidity in the air above sea surface. Condensation can be generated by high solar irradiance warming the air mass over cold marine waters in spring (stations in the southern North-Sea and in the eastern English Channel) or by moist Atlantic air, associated with rains, in summer when high blooms occur in the river plumes. Nevertheless, the determinant cause of error in these chlorophyll-rich waters is the excessive sensitivity of the algorithms based on the Blue/Green ratios. OC4 and OC5 derive the Chl-*a* concentration in clear water from the maximum ratio of $R(442)/R(555)$, $R(489)/R(555)$, $R(509)/R(559)$ where R is the remote-sensing reflectance, here for the MERIS wavelengths in nm. In practice, the maximum ratio $R(509)/R(555)$ is selected as the maximum ratio for Chl-*a* concentration above around 5 g m^{-3} . For concentration higher than 10 mg m^{-3} the sensitivity of the OCx algorithms to the $R(509)/R(555)$ ratio is very high and a switch to another algorithms making use of higher wavelengths is recommended to have better estimations in phytoplankton-rich waters [33,34].

4.1.3. Effect of the Sampling Volume on TSM and Turbidity

The small volume sampled *in situ*, of the order of $\frac{1}{2} L$, contrasts with the large volume observed from space. Short scales are therefore filtered out by the satellite method and the variance within the satellite dataset of a station is expected lower than its *in situ* counterpart (the so-called support effect in geostatistics). The support effect is prominent in the monitoring of TSM and turbidity at stations under the influence of small rivers, such as Boulogne Point 1. Boulogne Point 1 is more likely to be influenced by the nearby watershed (Liane river, Boulogne harbor) than the other stations in the eastern English Channel. Whereas the SRN transect was defined to assess anthropogenic impacts on phytoplankton dynamics, the SOMLIT transect was proposed as a reference for typical coastal waters away from anthropogenic pressures. In complement to the higher variability expected *in situ*, due to the support effect, there is also a higher error occurrence *in situ* in TSM that can be explained by a difficulty inherent to the measurement method. Remaining salts on the filter can cause an overestimation of TSM. The worst case is at Boulogne Point 1 where it appears very difficult to draw any conclusions from the *in situ* TSM datasets for 2017 as the SRN and SOMLIT stations exhibit contradictory results. Looking at the Turbidity graphs (Figure 5) can help us to identify possible artifacts in the TSM measurements at Boulogne Point 1. Indeed, the Turbidity graph corroborates the high values observed in TSM at Boulogne Point 1 (Figure 5a). At Boulogne Point 2 and 3, satellite and *in situ* turbidity values are very close and near average throughout the year. Regarding Boulogne Point 1, high levels in *in situ* TSM and turbidity observed in 2017 are not recorded in the 2016 and 2018 time series (Figure 12). Only two outliers can be noticed in the 2018 TSM graphs (Figure 12b). We may conclude that the 2017 case was not general at Boulogne Point 1 and that there is not a specific discrepancy between the sources of measurement (i.e., a satellite bias) at this location. It is also interesting to notice that there is a valuable signal in these time series in terms of coastal monitoring. For instance, the TSM and turbidity levels were clearly lower than average from March to June 2018 (Figure 12c,d). This was also observed at the other stations of the eastern English Channel (results not shown). The variability of the satellite retrievals in TSM and turbidity is generally lower than that observed *in situ* and some *in situ* outliers could be easily discarded by considering their deviation from the percentile curves and from the satellite retrievals. Therefore we can consider that the high range of variability in TSM measurements observed *in situ* may hamper the assessment of the statistics of the year (average and percentiles), suggesting that satellite imagery is more adapted for that purpose.

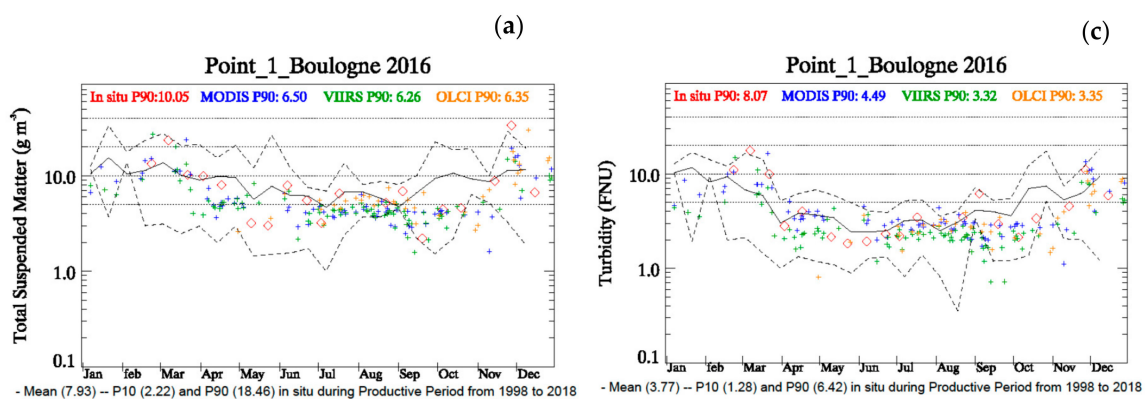


Figure 12. Cont.

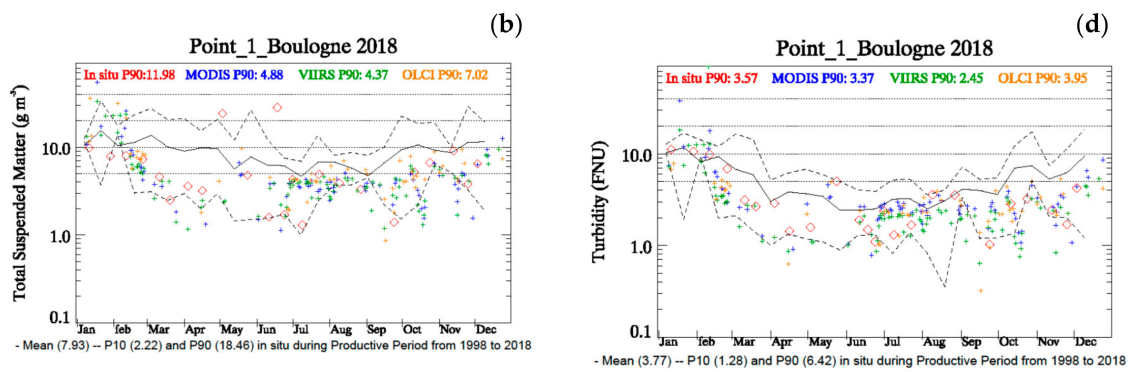


Figure 12. TSM (a,b) and Turbidity (c,d) at Boulogne Point 1 in 2016 and 2018.

4.1.4. Effect of the Sampling Volume on Chl-*a*

Chl-*a* and/or fluorescence (used as a proxy of Chl-*a*) appears to be less sensitive than turbidity and TSM to variability at small spatial scale, particularly in the river plumes. However, the variability within the water column can be high. The profiles in fluorescence, turbidity and temperature showed in Figure 13 provide a typical illustration of the conditions encountered in waters submitted to thermal stratification. A steadily increasing gradient of fluorescence is observed with depth. In that case a jump in the turbidity level is also observed between the first and second measurements, within a water layer one-meter depth. Integrating a deeper water column and a wider surface, the satellite method could provide more stable observations of Chl-*a* and turbidity (with higher levels in the conditions indicated on Figure 13).

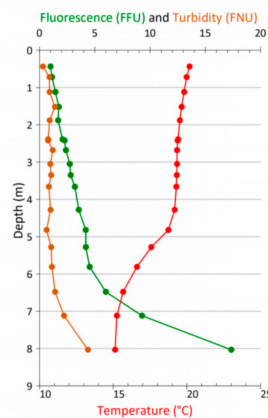


Figure 13. Fluorescence, Turbidity and Temperature profiles at Ouest-Loscolo on 19 June 2017. A general increase in fluorescence and turbidity is observed in relation to depth.

4.1.5. Effect of the Observation Time

In situ measurements are carried out around High Tide at the Atlantic stations whereas satellite products are recorded along sun-synchronous orbits with a repeat cycle of 16 days for MODIS and VIIRS and 27 days for OLCI-A aboard Sentinel-3. Although this has little effect on the Chl-*a* time series, a steady positive bias is exhibited by satellite TSM at the Antioche station. The location of this station in the Marennes-Oléron Bay is very particular and it is quite possible that the tidal cycle could play a major role in the bias exhibited by the satellite retrievals in TSM. The in situ sampling is made around High Tide whereas the satellite sampling, depending on sensors and orbits, could cover a wider range throughout the tidal cycle, including low tides with a higher concentration in TSM [35]. Surrounded by

intertidal areas with high TSM concentration, the station of Antioche could be particularly sensitive to the tidal cycle (Figure 14). Although all the satellite retrievals of the Atlantic stations are subject to this effect of complex aliasing, it is in TSM measurements and at Antioche that this latter effect is the most visible. A selection of images (MERIS or OLCI at 300 m resolution, MSI (Multi Spectral Imager) aboard Sentinel-2) corresponding to the exact times of the in situ observations could help clarifying this issue. Conversely to Atlantic waters, the tidal effect is weak at the Mediterranean stations. The excellent agreement achieved between the satellite and in situ Chl-*a* time series at Banyuls (Figure 10a) shows that the algorithm can perform remarkably when time effect is neglectable.

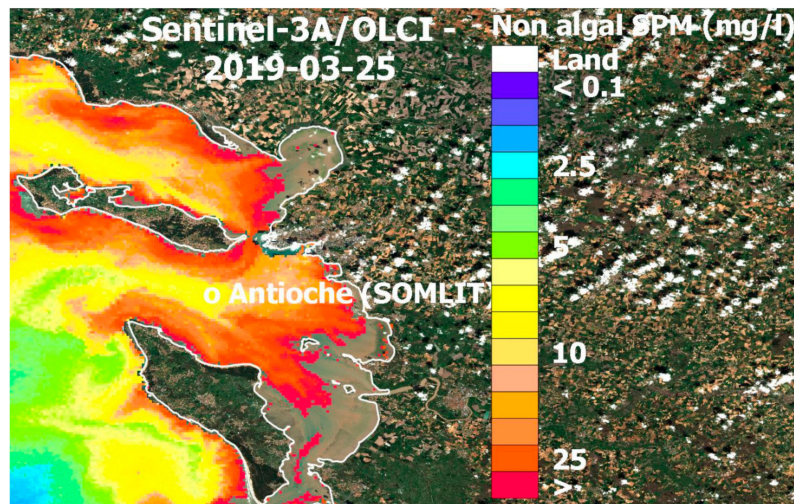


Figure 14. Non-algal SPM derived from OLCI-A at Antioche on 25 March 2019 at 12h10 UT (Low Tide at 12h47) Foreshore in brown.

4.2. Strategy for the Coastal Surveillance

The long-term surveillance, as requested by the European Directives and Regional Sea Convention, is based on indicators whose status is generally assessed every 6-year. A time period of 6 years enables the collection of a significant in situ dataset from which the ecological or environmental status of water bodies may be assessed. Every 6 years, the sampling network can also be re-organized in order to better evaluate the consequence of past or future measures implemented to improve the ecological status of the water bodies. Whereas a yearly assessment is not requested, a detailed yearly analysis should be of help to follow the reactivity of the ecosystem and trajectories of recovery after implementation of river basin management plan.

If in situ and satellite data are complementary for survey and research networks, there are nevertheless many pros and cons regarding in situ data as well as regarding satellite data. In situ data come from more direct measurement compared to satellite data and are usually considered to be reference data for calibrating satellite algorithms applied to marine reflectance. The in situ networks provide also a large panel of parameters (e.g., 16 parameters for the SOMLIT network) allowing a broad view of ecosystem functioning. However, in situ network, even if distributed over a few to several ecosystems sampled at one to a few stations, can only provide local information. Upscaling the data sets from the sampling stations to the whole ecosystem is usually not possible using in situ data only. In contrast, satellite data can give a view at spatial scales ranging from a local station to the global ocean [36]. Satellite can provide information at a daily time scale whereas in situ networks give information at weekly to monthly time scale, even if satellites are more sensitive to atmospheric conditions (cloud coverage) than research vessel to sea condition. At last, satellite remote-sensing is able to provide data in a repetitive fashion over areas not easily accessible using a research vessel at weekly to bimonthly frequency (e.g., continental shelves).

Our main results confirm the trend in lower Chl-*a* concentration after the spring bloom in the Eastern English Channel already discussed from long time series in [5]. The year 2017 is also characterized by a particularly low phytoplankton biomass in March at every station of the western coast (from the North-Sea to the Bay of Biscay). As this trend for lower Chl-*a* concentration in the English Channel is not accompanied with lower spring peaks it would be particularly useful to focus the in situ sampling on this season. That would paradoxically make more complex the estimation of the yearly P90, with an oversampling of the higher values in spring, but could lead to a better interpretation of the flora within the bloom context. The flora composition could be investigated from its position before, during, and after the peak of the bloom.

For the surveillance of the coastal environment, it is quite obvious that the satellite method enables a better overview of its spatial variability. Together with modeling [37–39], it is without equivalent on that point. The late winter blooms occurring offshore in the Bay of Biscay [40] and the *Karenia mikimotoi* blooms in the western English Channel [41,42] are not systematically observed from coastal stations. The spatial range of Turbidity over the continental shelf, not investigated in this study and poorly apparent from graphs at stations, is well observed in satellite imagery, particularly at the end of winter. In March, the spatial extent of turbidity resulting of winter storms reflects the consequence of low atmospheric pressures over western Europe that may affect large areas [43]. In contrast, detailed studies regarding e.g., the origin of particulate organic matter [22,23] or the long-term trends of phytoplankton diversity [44,45] would have not been possible using satellite data. Thus, satellite and in situ data sets are complementary and the combination of both data sets would be of great interest regarding research activities and surveillance in the scope of national and European frameworks.

4.3. Guidance to Improve and Develop the Satellite Method

4.3.1. A Switch to Higher Wave-Lengths in the Algorithm to Cope with High Chl-*a* Values

The overestimation of Chl-*a* observed in the nutrient-rich waters of the Eastern English Channel in spring and in the river plumes (Seine and Vilaine rivers) in spring and summer could be mitigated by switching to another satellite algorithm making use of channels in the Near-Infra-Red domain. Lavigne et al. [13] propose, for the eutrophic waters of the North-Sea, to switch from OC5 to the Gons algorithm [46] making use of the R(665) and R(705) channels available in the reflectance datasets of MERIS or OLCI-A. Another advantage of the Gons algorithm is that it is applicable to the high resolution images (20 m) of MSI (Multi Spectral Imager) aboard Sentinel2 and 3. With a channel at 705 nm, OLCI-A and OLCI-B reflectance can provide Chl-*a* products derived from a merged (OC5/Gons) algorithm whereas zooms could be available at 20 m resolution (but at lower frequency than at 1 km resolution) derived from MSI aboard Sentinel-2. However, this clear overestimation at the stations where strong blooms occur does not induce drastic consequences on P90 as the overestimated Chl-*a* are likely corresponding to true values over or around the percentile 90. That is why it was not observed a significant difference between in situ and satellite time series of P90 at Men er Roue and Ouest-Loscolo during the period 1998–2017 in [5].

4.3.2. Making Use of More Elaborate Satellite Products

If our aim is to estimate the inter-annual variability of Chl-*a* or TSM, then merged multi-sensor products [47] can be recommended. Figure 15 illustrates the capacity of the multi-sensor Chl-*a* product [48], used in [5], to exhibit the 2017 pattern at Boulogne Point 2. This product is easier to handle than the two VIIRS and MODIS products (Figure 4b). The merged product is smoother than reality (both in time and space) but is a good compromise for investing yearly or long-term trends.

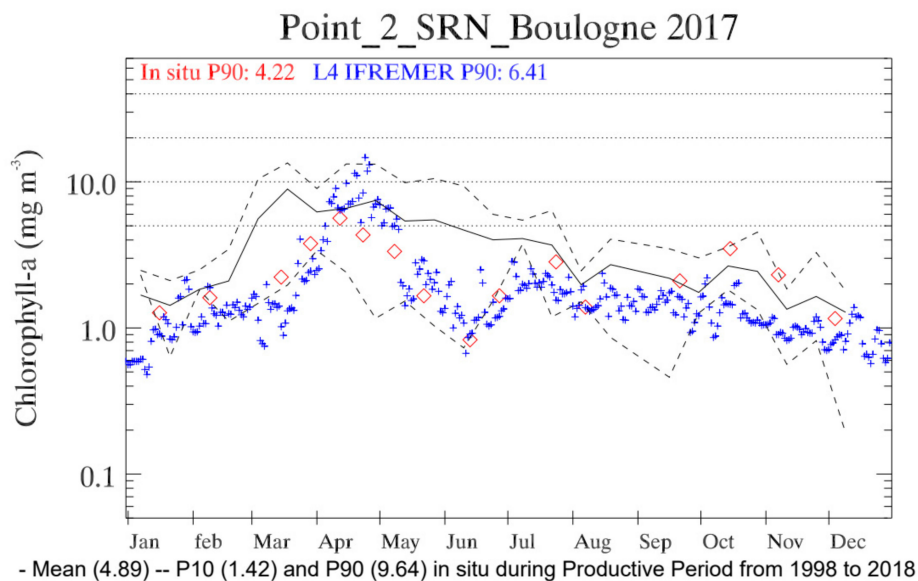


Figure 15. Merged Chl-*a* concentration derived from MODIS/VIIRS retrievals at Boulogne Point 2 in 2017.

4.3.3. A Large Panel of Products and Methods Available for Coastal Waters

There are indeed a large panel of potential products and satellite methods for coastal waters, mainly depending on their optical complexity. For the Wadden Sea, where CDOM cannot be neglected, Arabi et al. [49] propose an integrated multi-sensor and in situ monitoring, applying radiative transfer modeling to regional atmospheric and marine environments. In these conditions, MERIS aboard ENVISAT, OLCI, and MSI aboard Sentinel-2 provide high-quality remote-sensing reflectance that are managed together with a long time series of in situ hyperspectral measurements for monitoring Chl-*a*, TSM and CDOM. In waters optically less complex, as those that were studied here, and aiming at covering large regions encompassing the continental shelf, simplifications can be done in the processing of the satellite-derived reflectance.

Attempts are also made with success to identify phytoplankton functional types [50], phytoplankton size classes [51] and major phytoplankton groups [52], with a focus on Harmful Algal Blooms in coastal waters [53,54]. At the scale of the continental shelf, the most operational satellite product relative to phytoplankton species is the PIC (Particulate Inorganic Carbon) corresponding to coccolithophore blooms. The property of coccoliths to backscatter light has been used to develop operational algorithms for retrieving PIC from space in the clear waters of the open sea [55,56]. Coccolithophores are widely distributed over the continental shelf and at the shelf break, from the Bay of Biscay in April [57] to the Celtic Sea in June and the North-Sea in July and August. Despite their role in climate regulation, they are not a key phytoplankton group targeted in coastal monitoring as they are harmless and mainly occurring offshore but, belonging to the functional group of the calcifiers, they have a major ecological role.

5. Conclusions

Due to increasing anthropogenic pressures in a context of global warming, there is a steady development of integrated monitoring systems in coastal waters. In France, the SOMLIT network was initially in charge of long-term observations of coastal waters whereas the Ifremer REPHY was mainly dedicated to health risk and security in sea food. Since 2016, REPHY and SOMLIT share the monitoring of the phytoplankton diversity and abundance within the common PHYTOBS network aiming at achieving the long-term monitoring of phytoplankton along the French coasts [58].

Integration of satellite monitoring into conventional surveillance and observing systems is a complex task as satellites observe a few variables, compared to in situ measurements, performed at

coastal stations at low frequency or by instrumented buoys at high frequency. Our results indicate nevertheless an overall good agreement between satellite and in situ times-series of Chl-*a*, TSM and Turbidity, but also highlighted some discrepancies. These discrepancies are mainly due to differences in the volume (depth and area) of the sampling units and a time disparity in the data acquisition in tidal systems. Nevertheless, a better agreement can also be achieved by modifying the ocean color algorithm enabling a switch to higher wave-lengths in chlorophyll-rich waters or using merged products. However, the in situ measurements are not without uncertainties and the conventional networks could be improved in return by considering the satellite retrievals. Satellite and in situ observation systems are therefore complementary and merging their products for an operational and long-term monitoring of coastal waters is a major challenge for the next years. Among all the parameters available from space over the continental shelf, the first ones that could be candidates to this integrated monitoring are Chl-*a*, Turbidity and Total Suspended Matter.

Author Contributions: Conceptualization, F.G. and P.B.; software, P.B. and M.R.; resource, Y.B., T.C., P.C., S.C., G.C., S.F., A.G., A.P., T.H.F., M.L., A.P., P.R., M.R., V.V.; writing—original draft preparation, F.G., A.L., P.-G.S., N.S., T.H.F., V.V.; writing—review and editing, A.G., A.L., F.G., P.B., T.H.F., M.R., P.-G.S., N.S., V.V.; visualization, P.B., F.G., M.R. All authors have read and agreed to the published version of the manuscript.

Funding: This work was partly funded by the TELECHLOR project (Office Français de la Biodiversité and ARGANS-Ltd). It was also supported by the CNES/TOSCA OSYNICO project and the S-3 EUROHAB project funded by the European Regional Development Fund.

Acknowledgments: This study was carried out thanks to the long-term work of many people involved in the SOMLIT/REPHY monitoring networks and other supporting programs (SRN/RHLN . . .) providing freely available data. The authors also thank the space agencies for having provided marine spectral reflectances: the NASA Goddard Space Flight Center, Ocean Ecology Laboratory, Ocean Biology Processing Group for MODIS/AQUA, VIIRS data and ESA/EUMETSAT for Sentinel-3 (OLCI-A) and Sentinel-2 (MSI) data. We thank the three anonymous reviewers for their careful reading of our manuscript and their insightful comments and suggestions.

Conflicts of Interest: The authors declare no conflict of interest. The funders had no role in the design of the study; in the collection, analyses, or interpretation of data; in the writing of the manuscript, or in the decision to publish the results.

References

- O'Reilly, J.E.; Maritorena, S.; Mitchell, B.G.; Siegel, D.A.; Carder, K.L.; Garver, S.A.; Kahru, M.; McClain, C. Ocean color chlorophyll algorithm for SeaWiFS. *J. Geophys. Res.* **1998**, *103*, 24937–24953. [\[CrossRef\]](#)
- Gohin, F.; Saulquin, B.; Oger-Jeanneret, H.; Lozac'h, L.; Lampert, L.; Lefebvre, A.; Riou, P.; Bruchon, F. Towards a better assessment of the ecological status of coastal waters using satellite-derived Chlorophyll-*a* concentrations. *Remote Sens. Environ.* **2008**, *112*, 3329–3340. [\[CrossRef\]](#)
- Novoa, S.; Chust, G.; Sagarminaga, Y.; Revilla, M.; Borja, A.; Franco, J. Water Quality Assessment Using Satellite-Derived Chlorophyll-*a* within the European directives, in the southeastern Bay of Biscay. *Mar. Poll. Bull.* **2012**, *65*, 739–750. [\[CrossRef\]](#) [\[PubMed\]](#)
- Tilstone, G.; Mallor-Hoya, S.; Gohin, F.; Belo Couto, A.; Sá, C.; Goela, P.; Cristina, S.; Airs, R.; Icely, J.; Zühlke, M.; et al. Which Ocean colour algorithm for MERIS in North West European waters? *Remote Sens. Environ.* **2017**, *189*, 132–151. [\[CrossRef\]](#)
- Gohin, F.; Van der Zande, D.; Tilstone, G.; Eleveld, M.A.; Lefebvre, A.; Andrieux-Loyer, F.; Blauw, A.N.; Bryère, P.; Devreker, D.; Garnesson, P.; et al. Twenty years of satellite and in situ observations of Chlorophyll-*a* from the northern Bay of Biscay to the eastern English Channel. Is the water quality improving? *Remote Sens. Environ.* **2019**, *233*, 111343. [\[CrossRef\]](#)
- Lapucci, C.; Rella, M.A.; Brandini, C.; Ganzin, N.; Gozzini, B.; Maselli, F.; Massi, L.; Nuccio, C.; Ortolani, A.; Trees, C. Evaluation of empirical and semi-analytical chlorophyll algorithms in the Ligurian and North Tyrrhenian Seas. *J. Appl. Remote Sens.* **2012**, *6*. [\[CrossRef\]](#)
- Gómez-Jakobsen, F.; Mercado, J.M.; Cortés, D.; Ramírez, T.; Salles, S.; Yebra, L. A new regional algorithm for estimating chlorophyll-*a* in the Alboran Sea (Mediterranean Sea) from MODIS-Aqua satellite imagery. *Int. J. Remote Sens.* **2016**, *37*, 1431–1444. [\[CrossRef\]](#)

8. Mélin, F.; Vantrepotte, V.; Chuprin, A.; Grant, M.G.; Jackson, T.; Sathyendranath, S. Assessing the fitness-for-purpose of satellite multi-mission ocean color climate data records: A protocol applied to OC-CCI Chlorophyll-a data. *Remote Sens. Environ.* **2017**, *203*, 139–151. [CrossRef]
9. Garnesson, P.; Mangin, A.; Fanton d'Andon, O.; Demaria, J.; Bretagnon, M. The CMEMS GlobColour Chlorophyll-a product based on satellite observation: Multi-sensor merging and flagging strategies. *Ocean. Sci.* **2019**, *15*, 819–830. [CrossRef]
10. Gohin, F.; Druon, J.N.; Lampert, L. A five channel chlorophyll concentration algorithm applied to SeaWiFS data processed by SeaDAS in coastal waters. *Int. J. Remote Sens.* **2002**, *23*, 1639–1661. [CrossRef]
11. Gohin, F. Annual cycles of chlorophyll-a, non-algal suspended particulate matter, and turbidity observed from space and in situ in coastal waters. *Ocean. Sci.* **2011**, *7*, 705–732. [CrossRef]
12. Loisel, H.; Vantrepotte, V.; Ouillon, S.; Ngoc, D.D.; Herrmann, M.; Tran, V.; Mériaux, X.; Dessailly, D.; Jamet, C.; Duhaut, T.; et al. Assessment and analysis of the chlorophyll-a variability over the Vietnamese coastal waters from the MERIS ocean color sensor (2002–2012). *Remote Sens. Environ.* **2017**, *190*, 217–232. [CrossRef]
13. Lavigne, H.; Van der Zande, D.; Ruddick, K.; Cardoso Dos santos, J.; Gohin, F.; Brotas, V.; Kratzer, S. Quality-control tests for OC4, OC5 and NIR-red satellite chlorophyll-a algorithms applied to coastal waters. *Revis. Remote Sens. Environ.* **2020**, (In Press).
14. Common Procedure for the Identification of the Eutrophication Status of the OSPAR Maritime Area. Agreement 2013-08, 66p. Available online: <https://www.ospar.org/work-areas/hasec/eutrophication/common-procedure> (accessed on 25 August 2020).
15. Directive 2000/60/EC of the European Parliament and of the Council of 23 October 2000 Establishing a Framework for Community Action in the Field of Water Policy. *Off. J. Eur. Commun.* **2000**, *327*, 1–72.
16. Directive 2008/56/EC of the European Parliament and of the Council of 17 June 2008 establishing a framework for community action in the field of marine environmental policy (Marine Strategy Framework Directive). *Off. J. Eur. Commun.* **2008**, *164*, 19–40.
17. García-García, L.M.; Sivyver, D.; Devlin, M.; Painting, S.; Collingridge, K.; Van der Molen, J. Optimizing monitoring programs: A case study based on the OSPAR eutrophication assessment for UK waters. *Front. Mar. Sci.* **2019**, *5*, 503. [CrossRef]
18. SOMLIT. Service d'Observation en Milieu LITtoral Data. Available online: <https://www.somlit.fr/> (accessed on 25 August 2020).
19. REPHY—French Observation and Monitoring program for Phytoplankton and Hydrology in coastal waters. *REPHY Dataset—French Observation and Monitoring Program for Phytoplankton and Hydrology in Coastal Waters. 1987–2018 Metropolitan Data*; SEANO. 2019. Available online: <https://www.seano.org/data/00361/47248/> (accessed on 25 August 2020). [CrossRef]
20. SRN—Regional Observation and Monitoring program for Phytoplankton and Hydrology in the eastern English Channel. *SRN Dataset—Regional Observation and Monitoring Program for Phytoplankton and Hydrology in the Eastern English Channel, 1992–2016*; SEANO. 2017. Available online: <https://www.seano.org/data/00397/50832/> (accessed on 25 August 2020). [CrossRef]
21. Goffart, A.; Hecq, J.H.; Legendre, L. Drivers of the winter–spring phytoplankton bloom in a pristine NW Mediterranean site, the Bay of Calvi (Corsica): A long-term study (1979–2011). *Prog. Oceanogr.* **2015**, *137*, 121–139. [CrossRef]
22. Lienart, C.; Savoye, N.; Bozec, Y.; Breton, E.; Conan, P.; David, V.; Feunteun, E.; Grangere, K.; Kerherve, P.; Lebreton, B.; et al. Dynamics of particulate organic matter composition in coastal systems: A spatio-temporal study at multi-systems scale. *Prog. Oceanogr.* **2017**, *156*, 221–239. [CrossRef]
23. Liénart, C.; Savoye, N.; David, V.; Ramond, P.; Rodriguez, T.P.; Hanquiez, V.; Marieu, V.; Aubert, F.; Aubin, S.; Bichon, S.; et al. Dynamics of particulate organic matter composition in coastal systems: Forcing to the spatio-temporal variability at multi-systems scale. *Prog. Oceanogr.* **2018**, *162*, 271–289. [CrossRef]
24. Polsenaere, P.; Soletchnik, P.; Le Moine, O.; Gohin, F.; Robert, S.; Pépin, H.-F.; Stanisière, J.Y.; Dumas, F.; Béchemin, C.; Gouletquer, P. Potential environmental drivers of a regional blue mussel mass mortality event (winter of 2014, Breton Sound, France). *J. Sea Res.* **2017**, *123*, 39–50. [CrossRef]
25. Zurburg, W.; Smaal, A.; Héral, M.; Dankers, N. Seston dynamics and bivalve feeding in the bay of Marennes-Oléron (France). *Neth. J. Aquat. Ecol.* **1994**, *28*, 459–466. [CrossRef]

26. Yentsch, C.S.; Menzel, D.W. A method for the determination of phytoplankton chlorophyll and phaeophytin by fluorescence. *Deep Sea Res. Deep Sea Res. Oceanogr. Abstr.* **1963**, *10*, 221–231. [[CrossRef](#)]
27. Aminot, A.; Kérouel, R. *Hydrologie des écosystèmes Marins. Paramètres et Analyses*; Ifremer, Méthodes D'analyse en Milieu Marin; Editions Quae: Versailles, France, 2004; 336p, ISBN 2-84433-133-5.
28. Gohin, F.; Loyer, S.; Lunven, M.; Labry, C.; Froidefond, J.M.; Delmas, D.; Huret, M.; Herbland, A. Satellite-derived parameters for biological modelling in coastal waters: Illustration over the eastern continental shelf of the Bay of Biscay. *Remote Sens. Environ.* **2005**, *95*, 29–46. [[CrossRef](#)]
29. Jafar-Sidik, M.; Gohin, F.; Bowers, D.; Howarth, J.; Hull, T. The relationship between Suspended Particulate Matter and Turbidity at a mooring station in a coastal environment: Consequences for satellite-derived products. *Oceanologia* **2017**, *59*, 365–378. [[CrossRef](#)]
30. Van Heukelem, L.; Thomas, C.M.; Gilbert, P.M. *Sources of Variability in Chlorophyll Analysis by Fluorometry and High Performance Liquid Chromatography in a SIMBIOS Inter-Calibration Exercise*; NASA Technical Memorandum 2002-211606; Goddard Space Flight Center: Greenbelt, MD, USA, 2002.
31. Sathyendranath, S.; Lazzara, L.; Prieur, L. Variations in the spectral values of specific absorption of phytoplankton. *Limnol. Oceanogr.* **1987**, *32*, 403–415. [[CrossRef](#)]
32. Li, H.; He, X.; Shanmungam, P.; Bai, Y.; Wang, D.; Huang, H.; Zhu, Q.; Gong, F. Radiometric sensitivity and signal detectability of ocean color satellite sensor under high solar zenith angles. *IEEE Trans. Geosci. Remote Sens.* **2019**, *57*, 8492–8505. [[CrossRef](#)]
33. Dall'Olmo, G.; Gitelson, A.A.; Rundquist, D.C.; Leavitt, B.; Barrow, T.; Holz, J.C. Assessing the potential of SeaWiFS and MODIS for estimating chlorophyll concentration in turbid productive waters using red and near-infrared bands. *Remote Sens. Environ.* **2005**, *96*, 176–187. [[CrossRef](#)]
34. Smith, M.E.; Robertson Lain, L.; Bernard, S. An optimized chlorophyll *a* switching algorithm for MERIS and OLCI in phytoplankton-dominated waters. *Remote Sens. Environ.* **2018**, *215*, 217–227. [[CrossRef](#)]
35. Gernez, P.; Doxaran, D.; Barillé, L. Shellfish aquaculture from space: Potential of Sentinel2 to monitor tide-driven changes in turbidity, Chlorophyll concentration and oyster physiological response at the scale of an oyster farm. *Front. Mar. Sci.* **2017**, *4*, 137. [[CrossRef](#)]
36. Le Traon, P.Y.; Antoine, D.; Bentamy, A.; Bonekamp, H.; Breivik, L.A.; Chapron, B.; Corlett, G.; Dibarboue, G.; DiGiacomo, P.; Donlon, C.; et al. Use of satellite observations for operational oceanography: Recent achievements and future prospects. *J. Oper. Oceanogr.* **2015**, *8*, s12–s27. [[CrossRef](#)]
37. Druon, J.N.; Schrimpf, W.; Dobricic, S.; Stips, A. Comparative assessment of large-scale marine eutrophication: North Sea area and Adriatic Seas case studies. *Mar. Ecol. Prog. Ser.* **2004**, *272*, 1–23. [[CrossRef](#)]
38. Ferreira, J.G.; Andersen, J.H.; Borja, A.; Bricker, S.B.; Camp, J.; Cardoso da Silva, M.; Garcés, E.; Heiskanen, A.S.; Humborg, C.; Ignatiades, L.; et al. Overview of eutrophication indicators to assess environmental status within the European Marine Strategy Framework Directive. *Estuar. Coast. Shelf Sci.* **2011**, *93*, 117–131. [[CrossRef](#)]
39. Ménesguen, A.; Desmit, X.; Dulière, V.; Lacroix, G.; Thouvenin, B.; Thieu, V.; Dussauze, M. How to avoid eutrophication in coastal seas? A new approach to derive river-specific combined nitrate and phosphate maximum concentrations. *Sci. Total Environ.* **2018**, *628–629*, 400–414. [[CrossRef](#)] [[PubMed](#)]
40. Gohin, F.; Lampert, L.; Guillaud, J.F.; Herbland, A.; Nézan, E. Satellite and in situ observations of a late winter phytoplankton bloom, in the northern Bay of Biscay. *Cont. Shelf Res.* **2003**, *23*, 1117–1141. [[CrossRef](#)]
41. Vanhoutte-Brunier, A.; Fernand, L.; Menesguen, A.; Lyons, S.; Gohin, F.; Cugier, P. Modelling the *Karenia mikimotoi* bloom that occurred in the western English channel during summer 2003. *Ecol. Model.* **2008**, *210*, 351–376. [[CrossRef](#)]
42. Hartman, S.E.; Hartman, M.C.; Hydes, D.J.; Smythe-Wright, D.; Gohin, F.; Lazure, P. The role of hydrographic parameters, measured from a ship of opportunity, in bloom formation of *Karenia mikimotoi* in the English Channel. *J. Mar. Syst.* **2014**, *140*, 39–49. [[CrossRef](#)]
43. Gohin, F.; Bryère, P.; Griffiths, J.W. The exceptional surface turbidity of the North-West European shelf seas during the stormy 2013–2014 winter: Consequences for the initiation of the phytoplankton blooms? *J. Mar. Syst.* **2015**, *148*, 70–85. [[CrossRef](#)]
44. David, V.; Ryckaert, M.; Karpytchev, M.; Bacher, C.; Arnaudeau, V.; Vidal, N.; Maurer, D.; Niquil, N. Spatial and long-term changes in the functional and structural phytoplankton communities along the French Atlantic coast. *Estuar. Coast. Shelf Sci.* **2012**, *108*, 37–51. [[CrossRef](#)]

45. Hernandez-Fariñas, T.; Soudant, D.; Barillé, L.; Belin, C.; Lefebvre, A.; Bacher, C. Temporal changes in the phytoplankton community along the French coast of the eastern English Channel and the southern Bight of the North Sea. *ICES J. Mar. Sci.* **2013**, *71*, 821–833. [CrossRef]
46. Gons, H.J.; Rijkeboer, M.; Ruddick, K.G. A Chlorophyll-retrieval algorithm for satellite imagery (Medium Resolution Imaging Spectrometer) of inland and coastal waters. *J. Plankton Res.* **2002**, *24*, 947–951. [CrossRef]
47. Saulquin, B.; Gohin, F.; Garrello, R. Regional objective analysis for merging high-resolution MERIS, MODIS/Aqua, and seaWiFS Chlorophyll-*a* data from 1998 to 2008 on the European Atlantic shelf. *IEEE Trans. Geosci. Remote Sens.* **2011**, *49*, 143–154. [CrossRef]
48. Gohin, F. Chlorophyll-*a* Interpolée (Données Satellite); Ifremer. Available online: <https://sextant.ifremer.fr/record/9352f74a-7ecb-485e-8ea3-9aa91001b9a1/> (accessed on 25 August 2020). [CrossRef]
49. Arabi, B.; Salama, M.S.; Pitarch, J.; Verhoef, W. Integration of in-situ and multi-sensor satellite observations for long-term water quality monitoring in coastal areas. *Remote Sens. Environ.* **2020**, *239*, 111632. [CrossRef]
50. Moisan, T.A.; Rufty, K.M.; Moisan, J.R.; Linkswiler, M.A. Satellite observations of phytoplankton functional type spatial distributions, phenology, diversity, and ecotones. *Front. Mar. Sci.* **2017**, *4*, 189. [CrossRef]
51. Brewin, R.J.; Hardman-Mountford, N.J.; Lavender, S.J.; Raitsos, D.E.; Hirata, T.; Uitz, J.; Devred, E.; Bricaud, A.; Ciotti, A.; Gentili, B. An intercomparison of bio-optical techniques for detecting dominant phytoplankton size class from satellite remote sensing. *Remote Sens. Environ.* **2011**, *115*, 325–339. [CrossRef]
52. Alvain, S.; Moulin, C.; Dandonneau, Y.; Loisel, H. Seasonal distribution and succession of dominant phytoplankton groups in the global ocean: A satellite view. *Glob. Biogeochem. Cycles* **2008**, *22*. [CrossRef]
53. Kurekin, A.; Miller, P.; Van der Woerd, J. Satellite discrimination of *Karenia mikimotoi* and *Phaeocystis* harmful algal blooms in European coastal waters: Merged classification of ocean colour data. *Harmful Algae* **2014**, *31*, 163–176. [CrossRef]
54. Sourisseau, M.; Jegou, K.; Lunven, M.; Quere, J.; Gohin, F.; Bryere, P. Distribution and dynamics of two species of Dinophyceae producing high biomass blooms over the French Atlantic Shelf. *Harmful Algae* **2016**, *53*, 53–63. [CrossRef]
55. Balch, W.M.; Gordon, H.R.; Bowler, B.C.; Drapeau, D.T.; Booth, E.S. Calcium carbonate measurements in the surface global ocean based on Moderate-Resolution Imaging Spectroradiometer data. *J. Geophys. Res.* **2005**, *110*, C07001. [CrossRef]
56. Moore, T.S.; Dowell, M.D.; Franz, B.A. Detection of coccolithophore blooms in ocean color satellite imagery: A generalized approach for use with multiple sensors. *Remote Sens. Environ.* **2012**, *117*, 249–263. [CrossRef]
57. Perrot, L.; Gohin, F.; Ruiz-Pino, D.; Lampert, L.; Huret, M.; Dessier, A.; Malestroit, P.; Dupuy, C.; Bourriau, P. Coccolith-derived turbidity and hydrological conditions in May in the Bay of Biscay. *Prog. Oceanogr.* **2018**, *166*, 41–53. [CrossRef]
58. Cocquempot, L.; Delacourt, C.; Paillet, J.; Riou, P.; Aucan, J.; Castelle, B.; Charria, G.; Claudet, J.; Conan, P.; Coppola, L.; et al. Coastal ocean and nearshore observation: A French case study. *Front. Mar. Sci.* **2019**, *6*, 324. [CrossRef]

